

Supporting Information

Nickel-cobalt bimetallic tungstate decorated 3D hierarchical porous carbon derived from lignin for high-performance supercapacitor applications

Feiyan Shi^a [†], Shuai Zhao^c [†], Junyu Yang^b, Yao Tong^a, * Jiajun Li^a, Shangru Zhai^a,

Xinyu Zhao^a, Shenghan Wu^a, Hongsheng Li^a, Qingda An^a, *, Kai Wang^b, *

^a*Faculty of Light Industry and Chemical Engineering, Dalian Polytechnic University,*

Dalian 116034, Liaoning, China

^b*Dalian National Laboratory for Clean Energy; Dalian Institute of Chemical Physics,*

Chinese Academy of Sciences, Dalian 116023, China

^c*School of Science, Chongqing University of Technology, Chongqing 400054, China*

F. Shi and S. Zhao contributed equally to this work.

*Corresponding authors:

E-mail address: anqingdachem@163.com; wangkai@dicp.ac.cn;

tongyao@dlpu.edu.cn.

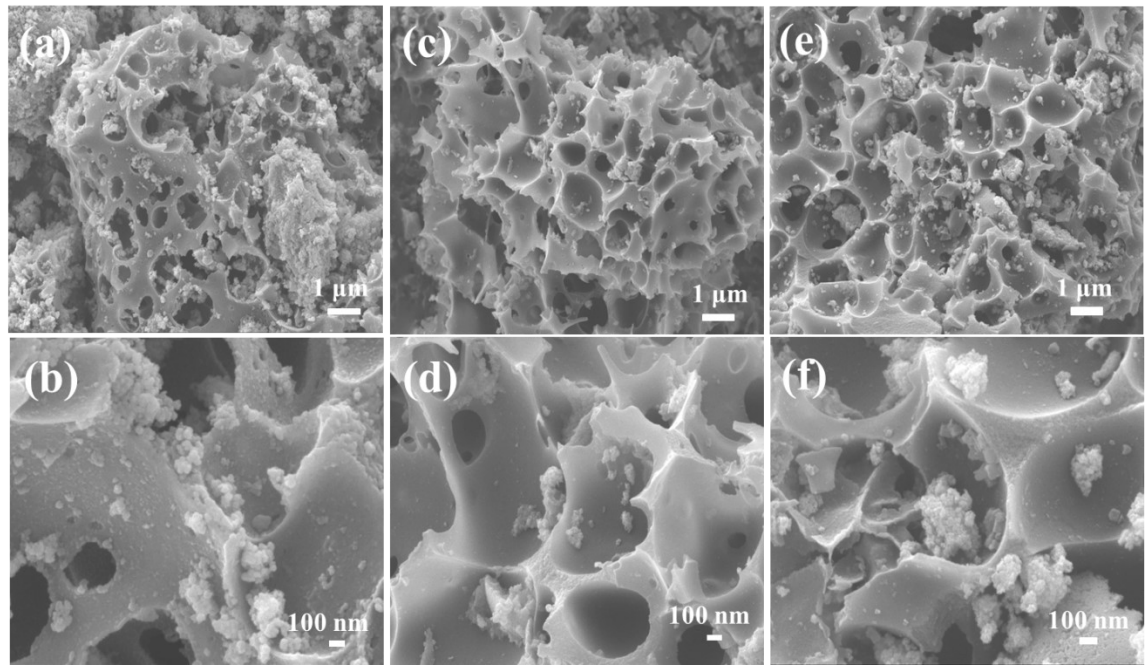


Fig. S1. (a) low and (b) high magnification SEM images of $\text{Ni}_{3.5}\text{Co}_{0.5}\text{WO}_4/\text{HPC}$; (c) low and (d) high magnification SEM images of $\text{Ni}_{2.5}\text{Co}_{1.5}\text{WO}_4/\text{HPC}$ and (e) low and (f) high magnification SEM images of $\text{Ni}_2\text{Co}_2\text{WO}_4/\text{HPC}$.

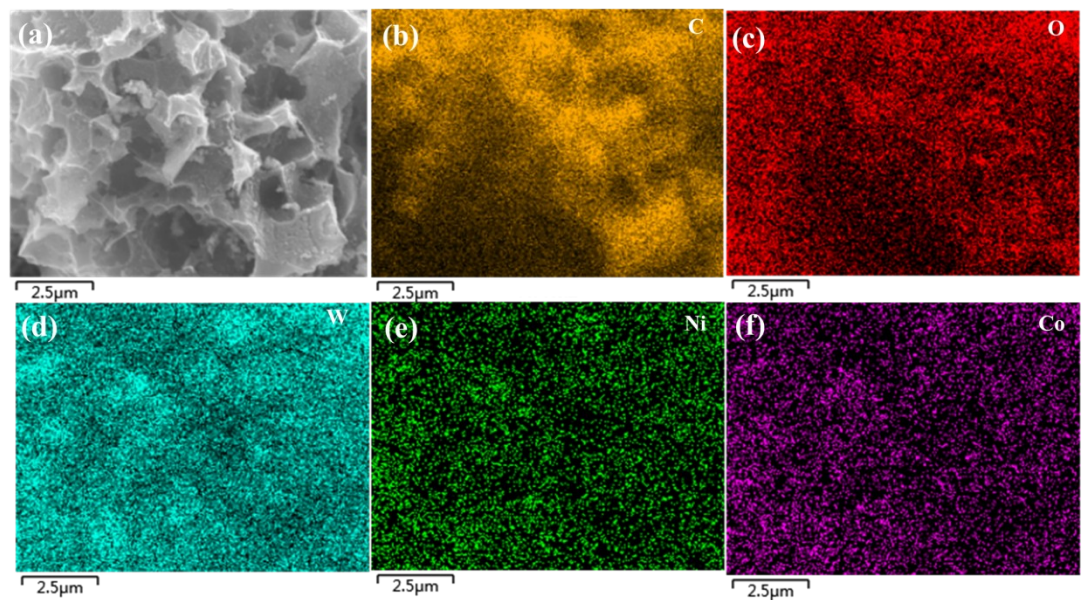


Fig. S2. (a) SEM images of the $\text{Ni}_3\text{Co}_1\text{WO}_4/\text{HPC}$, (b-f) EDS spectrum of $\text{Ni}_3\text{Co}_1\text{WO}_4/\text{HPC}$ nanocomposite.

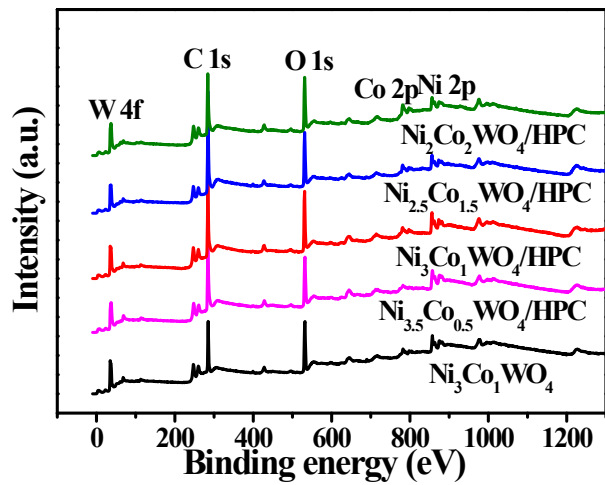


Fig. S3. The high resolution XPS spectra of Survey spectrum.

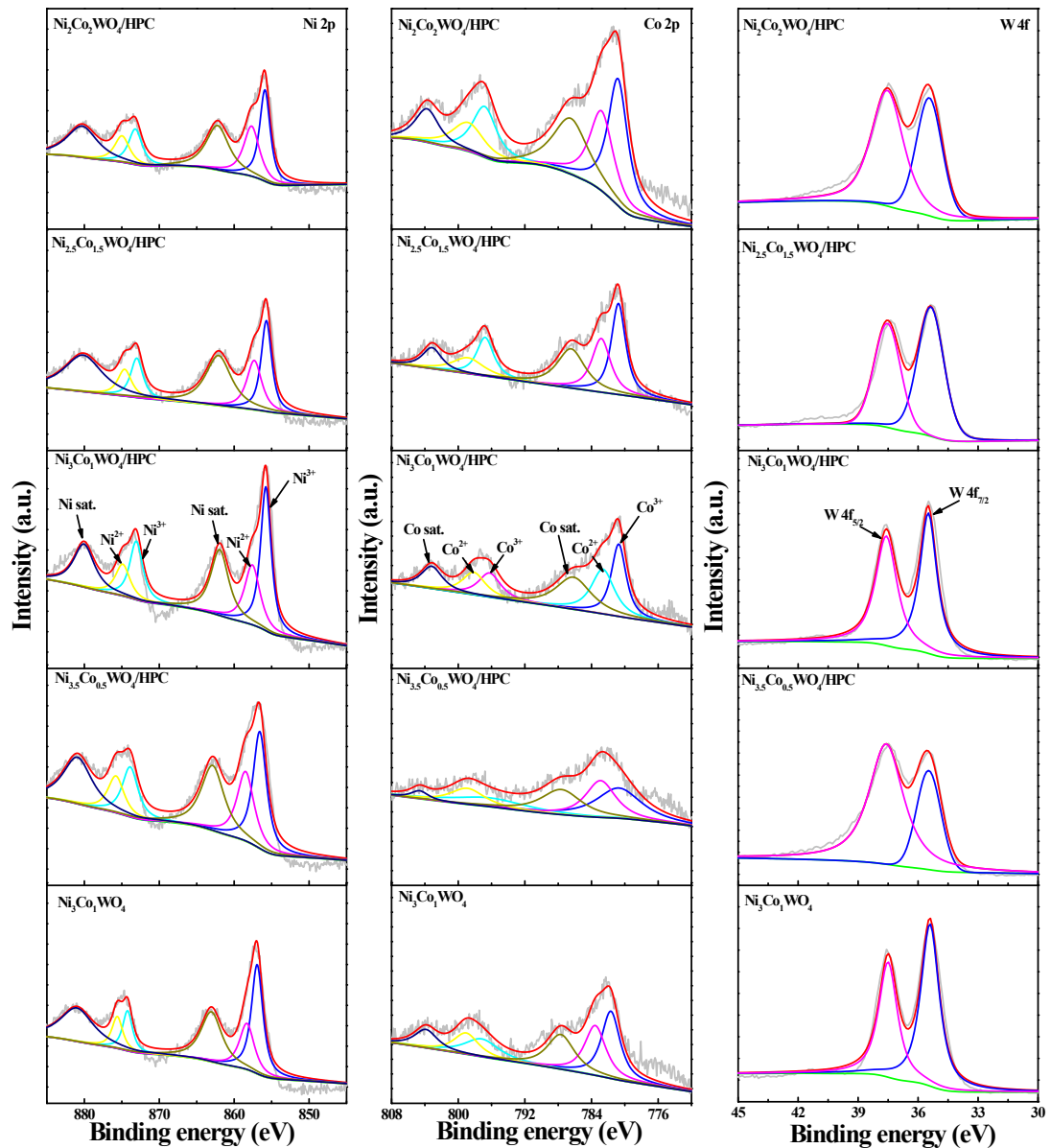


Fig. S4. High resolution XPS spectrum of Ni, Co and W in $\text{Ni}_{4-x}\text{Co}_x\text{WO}_4/\text{HPC}$ and $\text{Ni}_3\text{Co}_1\text{WO}_4$.

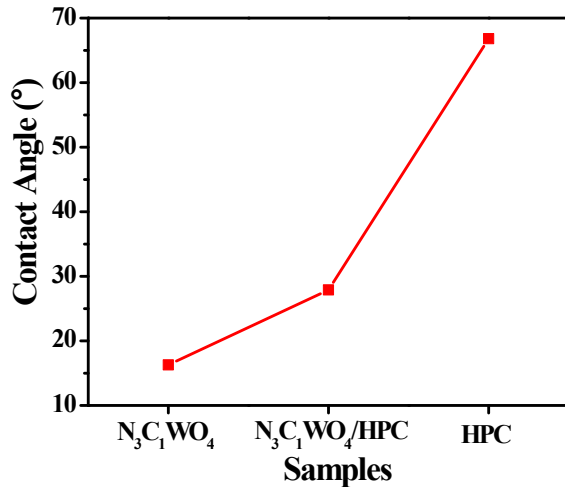


Fig.S5. The contact angles of the $\text{Ni}_3\text{Co}_1\text{W}$, $\text{Ni}_3\text{Co}_1\text{W}/\text{HPC}$ and HPC.

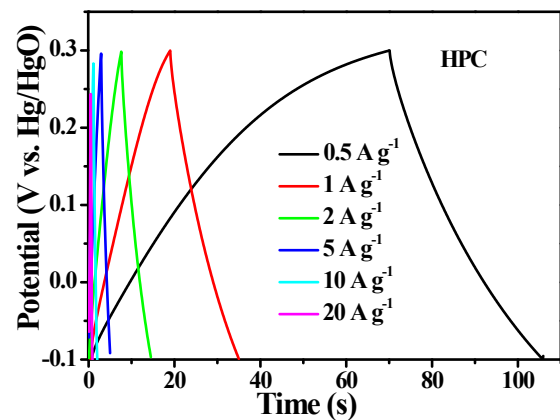


Fig.S6. GCD curves of HPC in a three-electrode system in 6 M KOH.

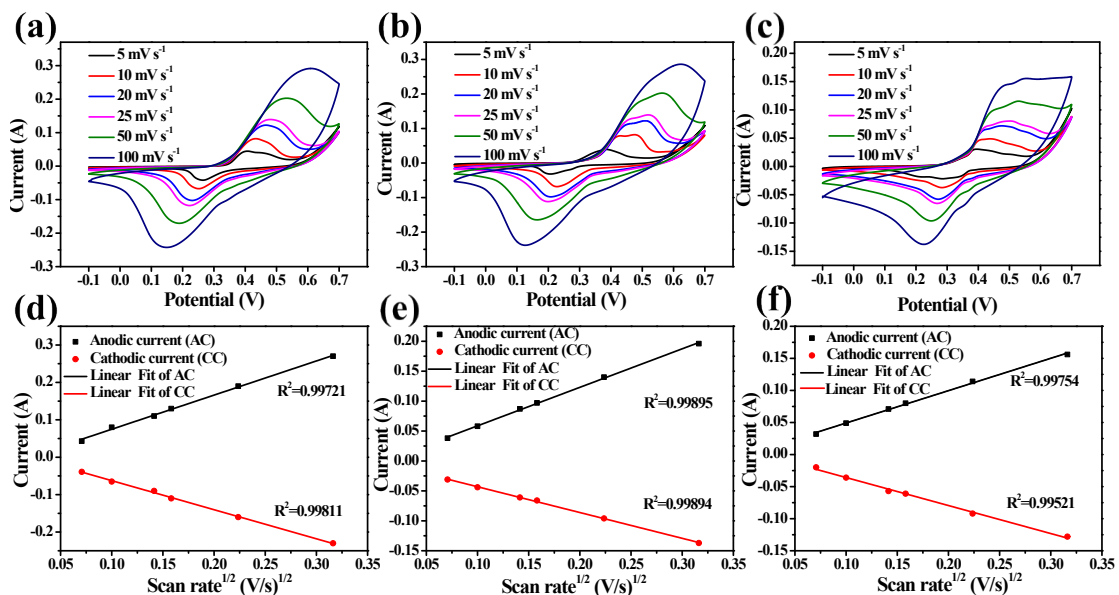


Fig. S7. CV curves at different scan rates of (a) $\text{Ni}_{3.5}\text{Co}_{0.5}\text{WO}_4/\text{HPC}$, (b) $\text{Ni}_{2.5}\text{Co}_{1.5}\text{ WO}_4/\text{HPC}$, (c)

$\text{Ni}_2\text{Co}_2\text{WO}_4/\text{HPC}$, the variation of the current of the cathodic and anodic peaks for the electrodes as a function of the square root of scan rate of (d) $\text{Ni}_{3.5}\text{Co}_{0.5}\text{WO}_4/\text{HPC}$, (e) $\text{Ni}_{2.5}\text{Co}_{1.5}\text{WO}_4/\text{HPC}$, and (f) $\text{Ni}_{2.5}\text{Co}_{1.5}\text{WO}_4/\text{HPC}$.

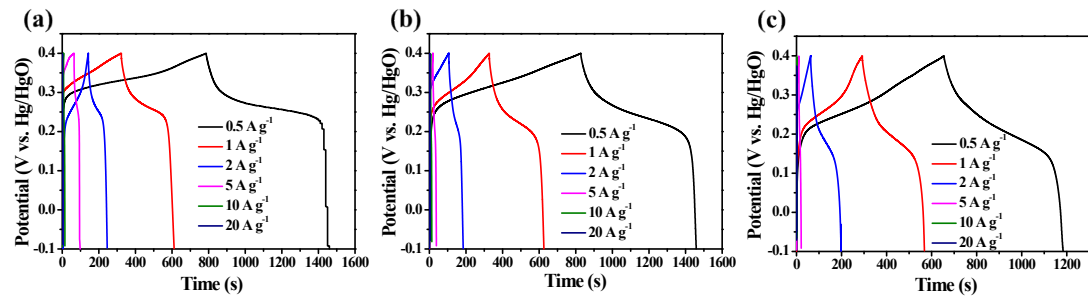


Fig.S8. GCD curves of (a) $\text{Ni}_{3.5}\text{Co}_{0.5}\text{WO}_4/\text{HPC}$, (b) $\text{Ni}_{2.5}\text{Co}_{1.5}\text{WO}_4/\text{HPC}$ and (c) $\text{Ni}_2\text{Co}_2\text{WO}_4/\text{HPC}$ determined in a three-electrode system in 6M KOH.

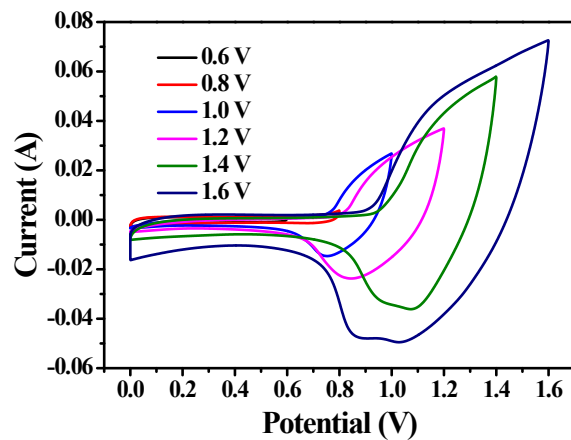


Fig.S9. CV curves of $\text{Ni}_3\text{Co}_1\text{W}/\text{HPC}$ nanocomposite in different potential windows in a two-electrode system in 6M KOH.

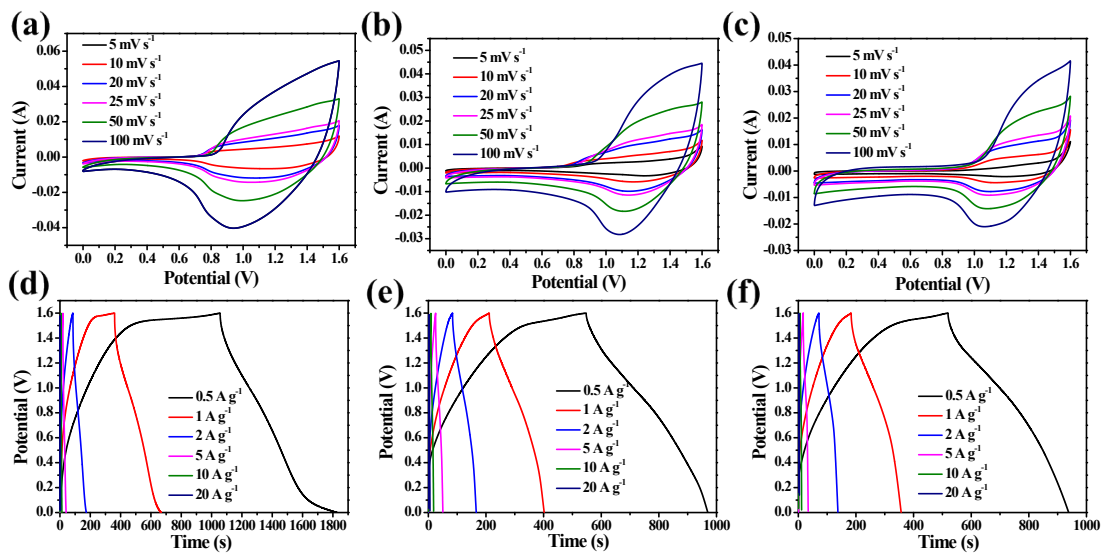


Fig.S10. CV curves of (a) $\text{Ni}_{3.5}\text{Co}_{0.5}\text{WO}_4/\text{HPC}$, (b) $\text{Ni}_{2.5}\text{Co}_{1.5}\text{WO}_4/\text{HPC}$ and (c) $\text{Ni}_2\text{Co}_2\text{WO}_4/\text{HPC}$, GCD curve of (d) $\text{Ni}_{3.5}\text{Co}_{0.5}\text{WO}_4/\text{HPC}$, (e) $\text{Ni}_{2.5}\text{Co}_{1.5}\text{WO}_4/\text{HPC}$ and (f) $\text{Ni}_2\text{Co}_2\text{WO}_4/\text{HPC}$ determined in a two-electrode system in 6M KOH.

Table S1. Pore textural properties of the pure NiCoWO₄ and NiCoWO₄/HPC composites.

Sample	S_{BET} ($\text{m}^2 \text{ g}^{-1}$)	S_{micro} ($\text{m}^2 \text{ g}^{-1}$)	V_{total} ($\text{cm}^2 \text{ g}^{-1}$)	V_{micro} ($\text{cm}^2 \text{ g}^{-1}$)
Ni ₃ Co ₁ WO ₄	53	-	0.086	-
Ni _{3.5} Co _{0.5} WO ₄ /HPC	282	49	0.44	0.021
Ni ₃ Co ₁ WO ₄ /HPC	300	91	0.38	0.041
Ni _{2.5} Co _{1.5} WO ₄ /HPC	281	76	0.29	0.034
Ni ₂ Co ₂ WO ₄ /HPC	235	75	0.33	0.033

Table S2. XPS of all the samples.

Samples	Ni ³⁺ (at %)	Ni ²⁺ (at %)	Ni ^{3+ /} Ni ²⁺	Co ³⁺ (at %)	Co ²⁺ (at %)	Co ^{3+ /} Co ²⁺	W (at %)
Ni ₃ Co ₁ WO ₄	5.01	2.74	1.83	1.9	1.62	1.17	5.42
Ni _{3.5} Co _{0.5} WO ₄ /HPC	3.32	1.66	2.00	0.75	0.61	1.23	2.82
Ni ₃ Co ₁ WO ₄ /HPC	3.29	1.99	1.65	0.96	0.92	1.04	2.81

Table S3. The fitted result of EIS data.

Sample	R_{ct}	R_s
Ni _{3.5} Co _{0.5} WO ₄ /HPC	0.54	0.44
Ni ₃ Co ₁ WO ₄ /HPC	0.47	0.36
Ni _{2.5} Co _{1.5} WO ₄ /HPC	0.96	0.45
Ni ₂ Co ₂ WO ₄ /HPC	1.26	0.45

Table S4. The OH⁻ diffusion coefficients in NiCoWO₄/HPC

Sample	Diffusion coefficients of OH ⁻ ($D_{\text{OH}^-} \times 10^{-8}/\text{cm}^2 \cdot \text{s}^{-1}$)	
	Ni ²⁺ /Ni ³⁺	Co ²⁺ /Co ³⁺ /Co ⁴⁺
Ni _{3.5} Co _{0.5} WO ₄ /HPC	7.38	4.65
Ni ₃ Co ₁ WO ₄ /HPC	7.95	5.01
Ni _{2.5} Co _{1.5} WO ₄ /HPC	5.2	3.28
Ni ₂ Co ₂ WO ₄ /HPC	4.08	2.57

Table S5. The comparison of the electrochemical property of various Co/Ni-based metal tungstates.

Nano-structure	Preparation method	Electrolyte	Sc (F·g ⁻¹ / C·g ⁻¹)	Specific current	Cycling stability	Ref.
NiWO ₄ nano-structure	Preparation method	2 M KOH	586.2	0.5 A·g ⁻¹	91.4% over 5000 cycles at 2 A·g ⁻¹	¹
RGO/CoWO ₄ nanocomposites	Hydrothermal	2 M KOH	159.9/112.0	5 mV·s ⁻¹	94.7 % over 1000 cycles at 1 A·g ⁻¹	²
CoWO ₄ @NiWO ₄ nanocomposites	Co-precipitation	1 M KOH	746/410	1 A·g ⁻¹	91.3 % over 2000 cycles at 2 A·g ⁻¹	³
NiWO ₄ /Ni foam nanostructures	Precipitation	2 M KOH	797.8/359.0	1 A·g ⁻¹	206 % over 6000 cycles at 50 mV·s ⁻¹	⁴
NiWO ₄ nanoparticles	Precipitation	2 M KOH	173/104	5 mV·s ⁻¹	90 % over 1000 cycles at 2 mA·cm ⁻¹	⁵
Co ₃ O ₄ @CoWO ₄ /rGO core–shell arrays	Hydrothermal- annealing	6 M KOH	386/193	0.5 A·g ⁻¹	\	⁶
NiWO ₄ /RGO nanocomposite	Solvothermal	2 M KOH	1031.3/618.8	0.5 A·g ⁻¹	100 % over 5000 cycles at 20 mV·s ⁻¹	⁷
NiWO ₄ -CoWO ₄ nanocomposite	Precipitation	2 M KOH	491.8/196.7	0.5 A·g ⁻¹	\	⁸
CoWO ₄ /NRGO	Situ sonochemical approach	2M H ₂ SO ₄	597	5 mV·s ⁻¹	97.1 % over 4000 cycles at 200 mV·s ⁻¹	⁹
CoWO ₄ nanoparticles	Hydrothermal- annealing	1 M H ₂ SO ₄	378/265	5 mV·s ⁻¹	95.5 % over 4000 cycles at 200 mV·s ⁻¹	¹⁰
CoWO ₄ @NiWO ₄ -A	Co-precipitation	1 M KOH	677.5	1 A·g ⁻¹	82 % over 5000 cycles at 5 A·g ⁻¹	¹¹
Co ₃ O ₄ /CoWO ₄ heterojunctions	Hydrothermal	6 M KOH	396.9	1 A·g ⁻¹	70.2 % over 2000 cycles at 7 A·g ⁻¹	¹²

Nano-structure	Preparation method	Electrolyte	Sc (F·g ⁻¹ / C·g ⁻¹)	Specific current	Cycling stability	Ref.
NiCo ₂ O ₄ @NiWO ₄ core-shell nanowire	Hydrothermal- annealing	6 M KOH	1384/692	1 A·g ⁻¹	87.6 % over 6000 cycles at 1 A·g ⁻¹	¹³
Ni _{0.85} Co _{0.15} WO ₄ Nanosheet	Co-precipitation	1 M KOH	360	0.1 A·g ⁻¹	\	¹⁴
NiWO ₄ nanowires	Solvothermal	6 M KOH	1190/595	0.5 A·g ⁻¹	\	¹⁵
CoNiWO ₄ /P-S-GNS nanocomposite	Hydrothermal	6 M KOH	1298.6	0.5 A·g ⁻¹	95.5 % over 7000 cycles	¹⁶
2D CNWO porous thin sheets	Hydrothermal	6 M KOH	1392/626.4	1 A·g ⁻¹	105.27 % over 10,000 cycles at 10 A·g ⁻¹	¹⁷
CoWO ₄ /Ni anocomposite	Co-precipitation	6 M KOH	271	1 A·g ⁻¹	86.4 % over 1,500 cycles at 5 A·g ⁻¹	¹⁸
Ni _{0.5} Co _{0.5} WO ₄	Hydrothermal	3 M KOH	34.55	1 A·g ⁻¹	92 % over 10,000 cycles at 10 A·g ⁻¹	¹⁹
NiWO ₄ nanoparticles	Hydrothermal	2 M KOH	427	1 A·g ⁻¹	99 % over 1000 cycles	²⁰
P-NiWO ₄ @CoWO ₄	Hydrothermal	6 M KOH	1683.4	1 A·g ⁻¹	84 % over 1000 cycles at 1 mA·cm ⁻¹	²¹
Ni₃Co₁WO₄/HPC	Co-precipitation	6 M KOH	1084	0.5 A·g⁻¹	80.74 % over 10,000 cycles at 10 A·g⁻¹	This work

References

1. Z. L. L Niu, Y Xu, J Sun, W Hong, X Liu, J Wang, and S Yang, *ACS Applied Materials Interface*, 2013, **5**, 8044-8052.
2. X. Xu, J. Shen, N. Li and M. Ye, *Electrochimica Acta*, 2014, **150**, 23-34.
3. X. Xu, J. Gao, G. Huang, H. Qiu, Z. Wang, J. Wu, Z. Pan and F. Xing, *Electrochimica Acta*, 2015, **174**, 837-845.
4. G. He, J. Li, W. Li, B. Li, N. Noor, K. Xu, J. Hu and I. P. Parkin, *Journal of Materials Chemistry A*, 2015, **3**, 14272-14278.
5. S. R. E. U Nithiyantham, S Anantharaj, and Subrata Kundu, *Crystal Growth & Design*, 2014, DOI: 10.1021/cg501366d.
6. Y. Y. Xiaowei Xu, Man Wang, Pei Dong, Robert Baines, Jianfeng Shen, Mingxin Ye, *Ceramics International*, 2016, DOI: 10.1016/j.ceramint.2016.03.192.
7. X. Xu, L. Pei, Y. Yang, J. Shen and M. Ye, *Journal of Alloys and Compounds*, 2016, **654**, 23-31.
8. C. S. Yidan Wang, Lengyuan Niu, Zhenkun Sun, Fengping Ruan, Man Xu, Shen Shan, Can Li, Xinjuan Liu, Yinyan Gong, *Materials Chemistry & Physics*, 2016, **182**, 394-401.
9. H. R. Naderi, A. Sobhani-Nasab, M. Rahimi-Nasrabadi and M. R. Ganjali, *Applied Surface Science*, 2017, **423**, 1025-1034.
10. K. Adib, M. Rahimi-Nasrabadi, Z. Rezvani, S. M. Pourmortazavi, F. Ahmadi, H. R. Naderi and M. R. Ganjali, *Journal of Materials Science: Materials in Electronics*, 2016, **27**, 4541-4550.
11. D. A. M Feng, H Zhang, G Ma, C Zhang and Z Ma, *International Journal of Chemical Studies*, 2017, **5**, 1954-1960.
12. X. Z. K Ding, J Li, P Yang, X Cheng, *ChemElectroChem*, 2017, **4**, 3011-3017.
13. S. Chen, G. Yang, Y. Jia and H. Zheng, *Journal of Materials Chemistry A*, 2017, **5**, 1028-1034.
14. Y. Huang, C. Yan, X. Shi, W. Zhi, Z. Li, Y. Yan, M. Zhang and G. Cao, *Nano Energy*, 2018, **48**, 430-440.
15. J. Tian, Y. Xue, X. Yu, Y. Pei, H. Zhang and J. Wang, *RSC Advances*, 2018, **8**, 41740-41748.
16. A. S. Rajpurohit, N. S. Punde, C. R. Rawool and A. K. Srivastava, *Chemical Engineering Journal*, 2019, **371**, 679-692.
17. B. Huang, H. Wang, S. Liang, H. Qin, Y. Li, Z. Luo, C. Zhao, L. Xie and L. Chen, *Energy Storage Materials*, 2020, **32**, 105-114.
18. K. Thiagarajan, D. Balaji, J. Madhavan, J. Theerthagiri, S. J. Lee, K. Y. Kwon and M. Y. Choi, *Nanomaterials (Basel)*, 2020, **10**.
19. S. Prabhu, C. Balaji, M. Navaneethan, M. Selvaraj, N. Anandhan, D. Sivaganesh, S. Saravanakumar, P. Sivakumar and R. Ramesh, *Journal of Alloys and Compounds*, 2021, **875**, 160066.
20. R. Packiaraj, P. Devendran, K. S. Venkatesh and N. Nallamuthu, *Inorganic Chemistry Communications*, 2021, **126**, 108490.
21. Q. H. Wenkang Miao, Hongming Zhang, Kangli Chen, Lu Zhang, Yuan Lia,* and S. H. , *Journal of Alloys and Compounds*, 2021, **877**, 160301.